AD_____

Award Number: W81XWH-11-1-0602

TITLE: In Vivo Imaging of Branched Chain Amino Acid Metabolism in Prostate Cancer

PRINCIPAL INVESTIGATOR: Daniel Spielman

CONTRACTING ORGANIZATION: Stanford University
Stanford, CA 94305

REPORT DATE: August 2013

TYPE OF REPORT: Annual

PREPARED FOR: U.S. Army Medical Research and Materiel Command
Fort Detrick, Maryland 21702-5012

REPORT DOCUMENTATION PAGE

Form Approved
OMB No. 0704-0188

1. REPORT DATE	2. REPORT TYPE	3. DATES COVERED
August 2013	Annual	15 July 2012 – 14 July 2013

4. TITLE AND SUBTITLE

In Vivo Imaging of Branched Chain Amino Acid Metabolism in Prostate Cancer

5a. CONTRACT NUMBER

5b. GRANT NUMBER
W81XWH-11-1-0602

5c. PROGRAM ELEMENT NUMBER

6. AUTHOR(S)

Daniel Spielman

E-Mail: spielman@stanford.edu

5d. PROJECT NUMBER

5e. TASK NUMBER

5f. WORK UNIT NUMBER

7. PERFORMING ORGANIZATION NAME(S) AND ADDRESS(ES)

Stanford University
Stanford, CA 94305

8. PERFORMING ORGANIZATION REPORT NUMBER

9. SPONSORING / MONITORING AGENCY NAME(S) AND ADDRESS(ES)
U.S. Army Medical Research and Materiel Command
Fort Detrick, Maryland 21702-5012

10. SPONSOR/MONITOR'S ACRONYM(S)

11. SPONSOR/MONITOR'S REPORT NUMBER(S)

12. DISTRIBUTION / AVAILABILITY STATEMENT
Approved for Public Release; Distribution Unlimited

13. SUPPLEMENTARY NOTES

14. ABSTRACT

The primary objective of this research effort is the development of noninvasive imaging method to assess branched-chain amino acid metabolism (known to be modified in prostate cancer [PC]) to distinguish malignant from healthy tissue. The approach is to use MRSI of hyperpolarized 13C-ketoisocaproic acid (KIC) to interrogate its conversion to leucine as catalyzed by branched-chain aminotransferase (BCAT). During this funding cycle, we:

1. Developed a high-throughput assay for assessing in vitro BCAT activity.
2. Demonstrated BCAT activity in TRAMP mouse models was significantly lower than that found in human PC.
3. Searched for an animal model more closely mimicking human metabolism by assessing four prostate cancer cell lines: PC-3, DU-145, LNCaP and LAPC-4. The PC-3 cells had the highest BCAT activity, although still appreciably lower than human PC.
4. Performed hyperpolarized in vivo MRS studies on PC-3 xenografts. Although the xenograph BCAT activity was 2.5 fold higher than cells alone (approaching human levels), the tumors grew very poorly (volumes ≤ 0.2 cc, as compared to the expected > 1 cc) and were inadequate to yield sufficient SNR for the in vivo MRS studies. 5. Initiated additional xenografts studies as well as investigation into other PC metabolic pathways.

15. SUBJECT TERMS
Hyperpolarized 13C-MRS, metabolism, imaging, KIC, leucine, branched-chain amino acid metabolism, BCAT

16. SECURITY CLASSIFICATION OF:			17. LIMITATION OF ABSTRACT	18. NUMBER OF PAGES	19a. NAME OF RESPONSIBLE PERSON
a. REPORT	b. ABSTRACT	c. THIS PAGE			USAMRMC
U	U	U	UU	15	19b. TELEPHONE NUMBER *(include area code)*

Table of Contents

In Vivo Imaging of Branched-Chain Amino Acid Metabolism in Prostate Cancer

Introduction

The primary objective of this research effort is the development a novel, non-invasive imaging technique that distinguishes malignant from healthy prostate tissue based upon their distinctive metabolic profiles. Our initial approach was to use MRSI of hyperpolarized ^{13}C-ketoisocaproic acid (KIC) to interrogate its conversion to leucine (Leu) as catalyzed by branched-chain aminotransferase (BCAT). Our primary finding, summarized under **Body: Hyperpolarized ^{13}C-KIC**, was that, despite the fact that BCAT activity is altered in prostate cancer relative to healthy tissue, insufficient enzymatic levels significantly limits the applicability of this biomarker to hyperpolarized ^{13}C MR spectroscopic imaging. As a result of our prostate cancer BCAT findings and in consultation with Army Contracting Officer Representative, Dr. Melissa Cunningham, we revised our Statement of Work with the inclusion of a new Aim focused on investigating new hyperpolarized ^{13}C-labeled substrates for the assessment of prostate cancer (see Appendix 1: Revised Statement of Work). Specifically, as part of these cell-culture and xenograph experiments we have identified several new PC metabolic pathways that may be assessable using hyperpolarized ^{13}C-MRS, and the new Aim is listed below, and initial results under this new Aim are described in **Body: Hyperpolarized ^{13}C-diethylsuccinate (DES)**.

Revised Aim: To assess the potential for novel hyperpolarized 13C-labeled substrates for in vivo magnetic resonance spectroscopic imaging of prostate cancer metabolism.

The completion of this Aim will include cell culture and in vivo studies in the currently being studied mouse (TRAMP) and rat (xenograph) models and will include studies of tumor grade and response to therapy using a castration model. Based on the approach presented below, we propose to study hyperpolarized 13C MRS markers of TCA cycle efficiency, inhibition of the glycolysis pathway, and oxidative stress.

Body

Hyperpolarized ^{13}C-KIC

Introduction

The recent advent of hyperpolarized ^{13}C MRS,[10] which achieves dramatically enhanced signal-to-noise ratios using dynamic nuclear polarization (DNP), provides unprecedented opportunities for real-time imaging of *in vivo* metabolic pathways critical to the identification and evaluation of cancer.[11] As first reported by Karlsson et al., [1-^{13}C]-2-ketoisocaproate ([1-^{13}C]-KIC) is a promising substrate for *in vivo* hyperpolarized ^{13}C MRS studies.[14] [1-^{13}C]-KIC is metabolized to [1-^{13}C]-leucine ([1-^{13}C]-Leu) by branched-chain aminotransferases (BCAT). In humans, BCAT has two major isoforms, BCAT1 (cytosol) and BCAT2 (mitochondria), and the enzyme also catalyzes the transamination of other BCAAs including isoleucine and valine.[15] BCAT, first identified as an overexpressed gene product in a mouse teratocarcinoma cell line,[16] is a target of the proto-oncogene *c-myc* and a putative marker for metastasis.[14,17] Following the bolus injection of hyperpolarized [1-^{13}C]-KIC, the metabolic production of [1-^{13}C]-Leu has been recently shown to correlate with BCAT levels in murine lymphoma (EL4), a tumor with high BCAT activity.[14]

Although as yet unstudied using hyperpolarized ^{13}C MRS techniques, recent reports have demonstrated the critical role of BCAAs in the proliferation of tumorgenic prostate tissue.[18] In particular, a variety of cancerous tissues are characterized by altered BCAA availability and elevated rates of BCAA oxidation.[19] BCAA metabolism is primarily altered in malignant tissue in order to meet the demands of *de novo* protein synthesis.[20] BCAAs can alternatively be utilized for energy production through a catabolic pathway mediated initiated by BCAT. Several other lines of evidence support the potential importance of BCAT metabolism in prostate cancer. In a recent clinical PET study, anti-1-amino-3-^{18}F-fluorocyclobutane-1-carboxylic acid (anti-^{18}F-FACBC), a synthetic leucine analog, was demonstrated to be a promising radiotracer for imaging prostate cancer with significant uptake in both primary and metastatic disease.[21] In this report, BCAT activity is investigated in various models of prostate cancer and the ability of hyperpolarized [1-^{13}C]-KIC to probe BCAA metabolism is explored.

Materials and Methods

Imaging Agent: The [1-^{13}C]-KIC free acid was prepared in a 96% yield (>99% purity) from the commercially available sodium salt, [1-^{13}C]-ketoisocaproic acid (Cambridge Isotopes, Andover, MA).[14]

Dynamic Nuclear Polarization of [1-^{13}C]-KIC: The samples to be polarized consisted of 20 μL of a mixture of 8 M [1-^{13}C]-KIC and 11 mM Ox063 trityl radical. Dotarem (1 μL of a 1:50 dilution, Guerbet, France) was added just prior to polarization. The samples were polarized via DNP using a HyperSense system (Oxford Instruments Molecular Biotools, Oxford, UK), for 1–1.5 h each, to achieve liquid-state polarization at dissolution of 15%. The polarized sample was initially dissolved in a buffered solution (80 mM NaOH mixed with 40 mM TRIS buffer, 50 mM NaCl and 0.1 g/L EDTA-Na_2) followed by further dilution with a solution (40 mM TRIS buffer, 50 mM NaCl and 0.1 g/L EDTA-Na_2) leading to a 4 mM solution of the hyperpolarized substrate with a pH of ~7.5.

Prostate Cancer Cell Lines: Prostate cancer cell lines (PC-3 and DU-145) were purchased from American Type Culture Collection (ATCC, Manassas, VA). LNCaP and LAPC-4 were generously donated by the Canary Center (Stanford University). Each cell line was cultured with Dulbecco's Modified Eagle Medium (DMEM) supplemented with 10% Fetal Bovine Serum (FBS) and 1% penicillin/streptomycin and grown to >80% confluence prior to *in vitro* studies.

Spectrophotometric BCAT assays: Homogenates were prepared from both healthy and malignant patient prostate tissues, and BCAT enzyme activity levels were determined spectrophotometrically via a previously reported protocol.[22] Human prostate tissue samples were donated by the Urology Department at Stanford University. A series of enzymatic assays were also performed with TRAMP mice, which were purchased from the Charles River Laboratories (Wilmington, MA). For cellular experiments, BCAT enzyme activities in the human prostate cancer cell lines (PC-3, DU-145, LNCaP and LAPC-4) were employed. Protein concentrations for each sample were determined via the Bradford assay.

Tumor induction: Human prostate cancer cell (PC-3) xenografts were induced on either flank of nu/nu nude mice Charles River Laboratories (Wilmington, MA) through the subcutaneous injection of 2-5 million cells in a PBS/matrigel (50:50) medium. PC-3-based xenografts showed relatively slow tumor progression *in vivo* and a growth rate of ~5 mm^3/day was observed.

MR experiments: *In vitro* MRS studies (n = 3 for each cell line) were conducted on the human prostate cancer cell lines utilizing a clinical 3T GE Signa MRI scanner (GE Healthcare, Waukesha, WI, USA). Immediately before dissolution, approximately 1x10^8 PC-3 or DU-145 cells were trypsinized and resuspended in 2 ml culture media. This was followed by an injection of 2 ml of 4 mM hyperpolarized [1-^{13}C]-KIC solution, which had been polarized using a HyperSense dynamic nuclear polarizer (Oxford Instruments Molecular Biotools, Oxford, UK). All MR measurements were performed using a custom-built carbon-13 surface coil ($\varnothing_{inner}$ = 28 mm), operating at 32.16 MHz, was used for both radiofrequency excitation and signal reception. Dynamic free induction decay spectroscopic sequence (spectral width, 5,000 Hz; spectral points, 2048) with hard RF pulse excitations (pulse width, 40μs; nominal flip angle, 10^o) was used to acquire spectra with 3 s of temporal resolution (total T_{acq} = 4:00 min).

The acquired data sets were apodized by a 10-Hz Gaussian filter and zero-filled by a factor of 4 in spectral dimension. After a fast Fourier transform (using MATLAB (Mathworks Inc., Natick, MA, USA), the metabolite peaks were integrated in absorption mode after zero-order phase correction to quantify time-curves of the metabolites. For the display of spectra, both a zero- and a first-order phase correction were performed and the baseline was subtracted by fitting a spline to the signal-free regions of the smoothed spectrum. [1-^{13}C]-Leu-to-[1-^{13}C]-KIC ratios were calculated by summing first 30 time-points (90 s) of each metabolite's time-curve and taking ratios of the metabolite signal intensities.

Results

In vitro assessment of BCAT Activity in human prostate tissue: Healthy prostate tissue was found to display modest levels of BCAT activity (2.96 ± 0.10 U/gram of protein) (Figure 1a). However, prostate cancer homogenates proved to have a significant decrease in enzyme activity as 1.68 ± 0.48 U/gram of protein was detected (P = 0.0045). Although BCAT activity is not at high levels in either state, this unique metabolic profile displayed by the malignant tissue could still be exploitable as a biomarker.

In vitro assessment of BCAT Activity in models of human prostate cancer: In *ex vivo* experiments, homogenates of TRAMP prostate tissues were found to possess an enzyme activity of 0.84 ± 0.17 U/gram of protein (Figure 1b); therefore, TRAMP mice display a decreased level of BCAT activity relative to human disease. In addition, a variety of human prostate cancer cell lines were examined in order to determine whether they would serve as appropriate models for spectroscopic studies. BCAT enzymatic assays were conducted with four cell lines: PC-3, DU-145, LNCaP and LAPC-4 (Figure 1c).[23] In these experiments, the human prostate cancer cell line, PC-3, displayed the highest level of BCAT activity (1.05 ± 0.39 U/gram of protein) followed by the DU-145 cell line (0.97 ± 0.16 U/gram of protein). Both were found to have increased enzyme activity in comparison to the TRAMP mouse model. Low levels of BCAT activity were detected *in vitro* from both the LNCaP and LAPC-4 cell lines.

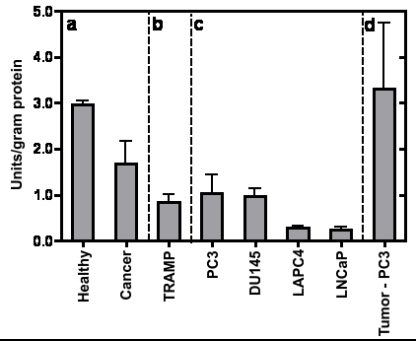

Figure 1. BCAT activity detected from the various prostate sources: (a) human, (b) TRAMP mouse model, (c) human prostate cancer cell lines and (d) PC-3 xenografts. Human prostate cancer displayed significantly lower levels of BCAT activity than normal tissue. Comparison of *in vitro* and *ex vivo* results obtained from PC-3 cell line after preparation of prostate cancer xenografts in immunocompromised nu/nu mice showed elevated enzyme activity levels after tumor induction.

Hyperpolarized ^{13}C MRS of human prostate cancer cell lines: Figure 2 displays averaged (a) spectra and (b) time-courses obtained after administration of hyperpolarized [1-^{13}C]-KIC to PC-3 cells in culture media (substrate concentration = 2 mM). In these experiments, [1-^{13}C]-KIC was observed at 172.6 ppm, and [1-^{13}C]-Leu was detected at 176.8 ppm. [1-^{13}C]-KIC•H_2O and [2-^{13}C]-KIC (natural abundance) were also present in the spectra but are not related to metabolism. The metabolic product, [1-^{13}C]-Leu, was immediately formed upon exposure of the prostate cancer cells to hyperpolarized [1-^{13}C]-KIC. The maximum product signal was detected after 15-20 s. Higher concentrations (up to 5 mM) of [1-^{13}C]-KIC did not result in increased product formation, which may suggest saturation of the BCAT active site at 2 mM. In addition, incubation (10 min) of cells with unlabelled leucine (1 mM) prior to analysis did not substantially affect [1-^{13}C]-Leu signal. Experiments were also performed with DU-145 cells and analogous metabolic products and time-courses were found (results not shown).

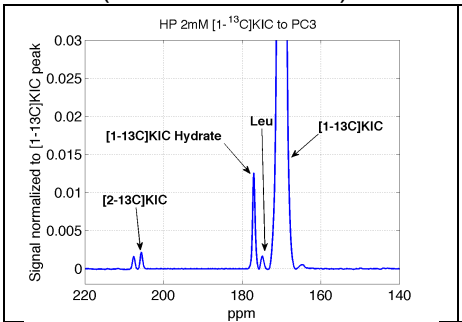

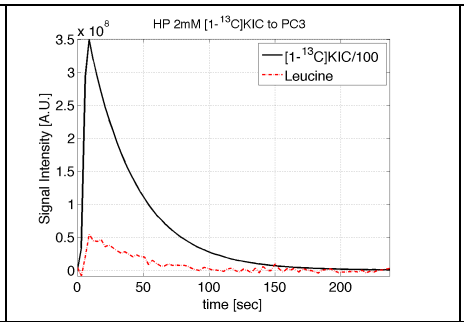

Figure 2. (a) Representative time-averaged spectra obtained from PC-3 prostate cancer cell line after incubation with of 2 mM [1-^{13}C]-KIC. (b) Representative time course demonstrate rapid uptake of hyperpolarized substrate and production of metabolic product, [1-^{13}C]-Leu.

Figure 3 summarizes the [1-^{13}C]-Leu-to-[1-^{13}C]-KIC ratios obtained for PC-3 and DU-145 cell lines from hyperpolarized ^{13}C MRS analysis. The metabolic product was observed over the first 100 s of the experiment, and PC-3 cells displayed a conversion ratio of 1.73 ± 0.38 a.u (mean ± ste, n = 3). [1-^{13}C]-Leu production and the area under the curve for this metabolic product were higher in DU-145 cells, and a 2.20 ± 0.47 ratio (mean ± ste, n = 3) was found. These results are consistent with our *in vitro* BCAT activity assays of these prostate cancer cell lines (Figure 1c). In addition, the [1-^{13}C]-Leu-to-[1-^{13}C]-KIC ratio provides a metric for evaluation of BCAT activity via hyperpolarized ^{13}C MRS.

Evaluation of BCAT activity in animal models of prostate cancer ex vivo: PC-3 xenografts were grown in immunocompromised nu/nu mice, and after euthanization, the tumors were examined *ex vivo* for BCAT activity. These results are summarized in Figure 1d. PC-3 xenografts displayed a 3.31 ± 1.43 U/gram of protein level of BCAT activity, which represents a >2.5-fold increase in enzyme activity in respect to the *in vitro* results. Similar elevated levels in tissues relative to the corresponding cell

lines have been observed in tumor models of murine lymphoma and rat mammary adenocarcinoma.[14] In addition, as part of this initial study of hyperpolarized [1-^{13}C]-KIC for analysis of BCAA metabolism in prostate cancer, preliminary *in vivo* studies were conducted with PC-3 xenografts as well as TRAMP mice (n = 2). However, despite the levels of BCAT activity found *ex vivo* for these tumor models, [1-^{13}C]-Leu production has yet to be observed *in vivo*.

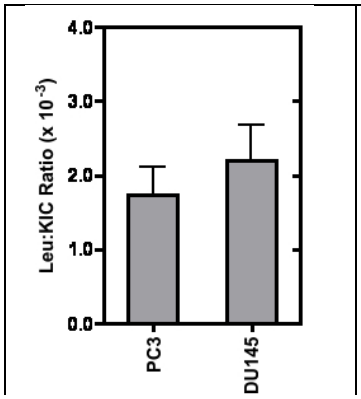

Figure 3. Metabolite ratio observed from *in vitro* hyperpolarized ^{13}C MR experiments with PC-3 and DU-145 prostate cancer cell lines. [1-^{13}C]-Leu-to-[1-^{13}C]-KIC ratio reflects the BCAT activity displayed in the respective cell lines.

Discussion

In this report, we investigated BCAT activity in several models of prostate cancer via both traditional and spectroscopic methods. While the work of Karlsson et. al. demonstrated the initial observation of metabolite formation from hyperpolarized [1-^{13}C]-KIC,[14] this study sought to validate [1-^{13}C]-KIC as a practical method for characterizing malignant prostate tissues. Through initial examination of BCAT activity *in vitro* via conventional spectrophotometric methods, we demonstrated that alterations in BCAA metabolism could assist in the evaluation of various prostate cancer models. In particular, healthy human prostate tissue was found to have an elevated BCAT levels relative to malignant tissue. Normal prostate tissue primarily relies upon fatty acid metabolism and glycolysis for energy production because the tricarboxylic acid (TCA) cycle is inhibited due to the high concentration of zinc. However, in prostate cancer, the TCA cycle is restored and can also contribute to meeting the energy requirements of the cell;[24] therefore, the observed changes in BCAT enzyme activity are in principle consistent with BCAAs being utilized for protein synthesis rather than for energy production.

Animal and cellular models are vital tools for exploring the onset and progression of human disease. In addition, a sufficient model, which maintains comparable rates of BCAT activity as human prostate cancer, was necessary for spectroscopic evaluation with hyperpolarized [1-^{13}C]-KIC. However, there remain a limited number of reports concerning alterations in BCAA demand and metabolism in models of prostate cancer. Through the initial spectrophotometric examination of the TRAMP mouse and prostate cancer cell lines, PC-3 and DU-145 cell lines were discovered to have similar BCAT activity levels as detected in human disease. These models were then employed in the development of ^{13}C MRS techniques for analyzing BCAA metabolism with hyperpolarized [1-^{13}C]-KIC in prostate cancer. To this end, we demonstrated that hyperpolarized [1-^{13}C]-KIC could be employed *in vitro* for models of prostate cancer. In both the PC-3 and DU-145 cell lines, BCAT activity was successfully examined through measuring [1-^{13}C]-Leu production after administration of the molecular probe. In the validation of this technique, we correlated our spectroscopically determined BCAT activities (reflected in [1-^{13}C]-Leu-to-[1-^{13}C]-KIC ratio) with those detected via standard spectrophotometric methods. The agreement of these results further validates the probe as measuring BCAT activity and supports [1-^{13}C]-KIC as a tool assessing of BCAT activity in models of prostate cancer. Importantly, this [1-^{13}C]-Leu-to-[1-^{13}C]-KIC ratio provides direct insight into the state of BCAA metabolism and, specifically, the propensity for BCAA oxidation, a pathway that can be utilized to drive energy production in proliferating cells.

Based upon our analysis, BCAA metabolism is altered in human prostate cancer relative to healthy tissue. However, only low levels of BCAT activity were found in all animal and cellular models examined. Despite these modest activities, we have successfully demonstrated that BCAT activity can be determined with hyperpolarized ^{13}C MRS *in vitro* using [1-^{13}C]-KIC, and the ratio of metabolite product to substrate ([1-^{13}C]-Leu-to-[1-^{13}C]-KIC) could be used as metric for monitoring changes in metabolic state. These spectroscopic results were further correlated with traditional *in vitro* assays. However, despite the fact that BCAT activity is altered in prostate cancer relative to healthy tissue, insufficient enzymatic levels significantly limit the potential use of this biomarker for hyperpolarized ^{13}C MR spectroscopic imaging *in vivo*.

Hyperpolarized ^{13}C-DES

Introduction

The tricarboxylic acid cycle (TCA) performs an essential role in the regulation of energy and metabolism, and deficiencies in this pathway are commonly correlated with various diseases. However, the development of non-invasive techniques for the assessment of the cycle *in vivo* has remained challenging. In this work, the applicability of a novel imaging agent, [1,4-^{13}C]-diethylsuccinate, for hyperpolarized ^{13}C metabolic imaging of the TCA cycle was explored. *In vivo* spectroscopic studies were conducted in conjunction with *in vitro* analyses to determine the metabolic fate of the imaging agent. Contrary to previous reports (Zacharias, N. M. et. al. *J. Am. Chem. Soc.* **2012**, *134*, 934-943)(3225), [^{13}C]-labeled diethylsuccinate was primarily metabolized to succinate-derived products not originating from TCA cycle metabolism. These results illustrate potential issues of utilizing dialkyl ester analogs of TCA cycle intermediates as molecular probes for hyperpolarized ^{13}C metabolic imaging.

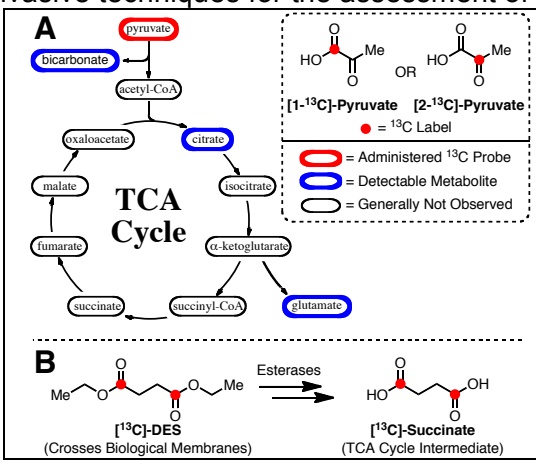

Figure 1. (A) Overview of compounds related to the TCA cycle that are generally detected when employing hyperpolarized [1-^{13}C]- or [2-^{13}C]-pyruvate. (B) Strategy for probing TCA cycle metabolism. DNP substrate, [^{13}C]-DES, enters intracellular environment and is converted into TCA cycle intermediate.

Experimental Details

General: All reagents were purchased from Aldrich Chemical Co. unless otherwise noted and used without further purification.

Synthesis of [1,4-^{13}C]-Diethylsuccinate: [^{13}C]-DES was prepared by the following procedure: In an oven-dried 100 mL round-bottom flask equipped with magnetic stir bar, 425 mg (3.54 mmol) of [1,4-^{13}C]-succinic acid (99% 1,4-^{13}C, CLM-1084, Cambridge Isotopes, Andover, MA) was added. After the addition of anhydrous ethanol (35 mL), 1.8 mL (1.54 g, 14.2 mmol) of trimethylsilyl chloride was added dropwise via syringe over the course of two minutes. The reaction was allowed to stir at room temperature. After 5 h, the reaction was quenched with 10 mL of saturated sodium bicarbonate solution. Additional bicarbonate was removed via filtration, and ethanol was removed under vacuum. The desired product was extracted from the aqueous solution with 4 x 8 mL of dichloromethane. Organic layers were combined, dried over anhydrous sodium sulfate, and filtered; the solvent was removed by evaporation and 480 mg (77% yield) of pure product was isolated as a colorless oil. ^{1}H NMR ($CDCl_3$, 500 MHz) δ 4.15 (q, *J* = 7 Hz, 4H), 2.60 (s, 4H), 1.12 (t, *J* = 7 Hz, 6H) ppm; ^{13}C NMR ($CDCl_3$, 125 MHz) δ 172.4, 60.8, 29.1, 14.1 ppm.

Synthesis of [1,4-^{13}C]-Monoethylsuccinate: In order to reference [^{13}C]-MES, a sample containing [^{13}C]-succinate, [^{13}C]-MES, and [^{13}C]-DES was prepared by the following procedure: In an oven-dried 100 mL round-bottom flask equipped with magnetic stir bar, 100 mg (0.83 mmol) of [1,4-^{13}C]-succinic acid was added. After the addition of anhydrous ethanol (5 mL), 0.106 mL (90.5 mg, 0.83 mmol) of trimethylsilyl chloride was added dropwise via syringe over the course of one minute. The reaction was allowed to stir at room temperature. After 30 min, the reaction was quenched with 2 mL of saturated sodium bicarbonate solution. Additional bicarbonate was removed via filtration, and ethanol was removed under vacuum. The desired product was extracted from the aqueous solution with 4 x 4 mL of dichloromethane. Organic layers were combined, dried over anhydrous sodium sulfate, and filtered; the solvent was removed by evaporation to yield a sample with 2:3:6 ratio of [^{13}C]-succinate:[^{13}C]-DES:[^{13}C]-MES as determined by ^{1}H-NMR (D_2O).

Dynamic Nuclear Polarization of [1,4-^{13}C]-Diethylsuccinate: The samples to be polarized consisted of 40 μL of a mixture of [^{13}C]-DES (6 M, neat) and 20-mM α,γ-Bisdiphenylene-β-phenylallyl (BDPA) radical. The samples were polarized via dynamic nuclear polarization using a HyperSense system (Oxford Instruments Molecular Biotools, Oxford, UK). The polarized samples were dissolved in a solution of 40-mM TRIS buffer, 50-mM NaCl and 0.1 g/L EDTA-Na_2, leading to an 80-mM solution of

the hyperpolarized substrate with a pH of approximately 7.5.

In Vivo Experiments: Healthy male Wistar rats (393 ± 48 g body weight, n = 3) were injected with 2.6-3.2 mL of the hyperpolarized solution (target dose = 1 mmol/kg body weight) through a tail vein catheter at a rate of approximately 0.25 mL/s. The time from dissolution to start of injection was approximately 20 s.

The rats were anesthetized initially with 2.5% isoflurane in oxygen (1.5 L/min) for tail vein catheterization. Respiration, rectal temperature, heart rate and oxygen saturation were monitored throughout the experiments with temperature regulated using a warm water blanket placed underneath the animals. Each animal received two injections of the hyperpolarized substrate, approximately 1.5 - 2 h apart. All animal procedures were approved by the SRI Institutional Animal Care and Use Committee.

All experiments were performed on a clinical 3T Signa MR scanner (GE Healthcare, Waukesha, WI), using a custom-built ^{13}C transmit/receive surface coil (dia = 28 mm) placed over the heart with rat supine. A quadrature volume rat ^{1}H coil (diameter = 70 mm) was used for anatomical localization and to confirm the position of the ^{13}C coil with respect to the heart. Single-shot fast spin-echo (FSE) ^{1}H MR images in the axial, sagittal and coronal planes with nominal in-plane resolution of 0.47 mm and 2-mm slice thickness were acquired as anatomical references for prescribing the ^{13}C MRS experiments. A non-selective pulse-and-acquire sequence with an excitation flip angle of 6°, spectral width of 5 kHz and 2048 points was used to acquire ^{13}C spectra from the heart every 3 s over a 4-min period starting at the same time as the [^{13}C]-DES injection.

In Vitro Experiments: *In vitro* experiments were performed in order to facilitate the identification of the metabolites observed from [^{13}C]-DES *in vivo* experiments. These experiments include exposure of [^{13}C]-DES to:

(1) Pig Liver Esterase. [^{13}C]-DES (10 mM) was incubated at 37 °C with pig liver esterase (7.5 Units/mL) in RPMI media supplemented with 10% fetal bovine serum and 5% penicillin-streptomycin. Pig liver esterase has been previously shown to selectively cleave a single ester of DES (3926). After 5 min, the solution was then analyzed via ^{13}C-NMR on an 11.7 T instrument to determine the product distribution.

(2) Rat blood. Blood draws were performed from healthy male Wistar rats via tail vein catheter. The freshly drawn blood (1 mL) was immediately dosed with [^{13}C]-DES (100 mM) and the solution was incubated at 37 °C. At various times points (1, 5, 20 and 60 min), a 0.25 mL aliquot of the solution was removed, and the sample was quenched with methanol (0.25 mL). Each sample was then analyzed via ^{13}C-NMR on an 11.7 T instrument to determine the metabolic fate of [^{13}C]-DES.

(3) Homogenates of Rat Heart. Rat hearts were obtained from male Wistar rats and samples were maintained at -80 °C. Samples were thawed, homogenized in buffer (210 mM mannitol, 70 mM sucrose, 5 mM MOPS and 1 mM EDTA in D_2O), and centrifuged at 3000*g* to obtain desired homogenates. These homogenates were dosed with [^{13}C]-DES (10 mM) and incubated at 37 °C for 5 min. These samples were analyzed at various time points (5, 20, 60 and 300 min) via ^{13}C-NMR on an 11.7 T instrument to determine the product distribution.

Results and Discussion

[^{13}C]-DES was successfully formulated for dynamic nuclear polarization through the addition of 20 mM BDPA to 6 M [^{13}C]-DES (neat). The solid-state polarization build-up time constant was 1517 ± 91 s (n = 8) with a liquid-state polarization level of 5.5% (Figure 2). The T_1 (^{13}C-labeled carbonyls) was found to be 37.9 s in solution at 3 T. No observable toxicity (pulse or respiration) was detected upon i.v. administration of a TRIS-buffered solution containing up to 80 mM [^{13}C]-DES. In addition, no detectable ester hydrolysis of [^{13}C]-DES to yield [1,4-^{13}C]-monethylsuccinate ([^{13}C]-MES) or [1,4-^{13}C]-succinate was observed when [^{13}C]-DES was exposed to the dissolution conditions (40-mM TRIS buffer, 50-mM NaCl and 0.1 g/L EDTA-Na_2, pH = 7.5) for a period of up to 20 min. Furthermore, no hydrolysis was observed during the dissolution process, which requires superheating the frozen sample (see supporting information).

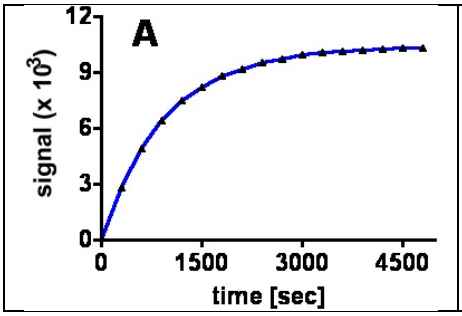

Figure 2. (A) Polarization buildup curves (3.35 T, 1.4 K) of [^{13}C]-DES doped with 20 mM BDPA taken at P(+) = 94.116 GHz. (B) Liquid-state T_1 decay (3 T, 298 K) of [^{13}C]-DES samples with 20 mM BDPA (T_1 = 38 s).

Figure 3 displays a representative (A) spectrum and (B) time-resolved stackplot obtained from a rat heart after i.v. administration of hyperpolarized [^{13}C]-DES. In these experiments, a bolus injection of 80 mM [^{13}C]-DES was performed, and the substrate was observed at 176.4 ppm along with three other distinct signals at 182.5, 177.6, and 172.7 ppm. Lower substrate concentration (40 mM) did not significantly affect metabolites observed or the relative quantities detected. Importantly, our spectra closely resembled the previously observed product distribution found in the report by Zacharias et. al. on PHIP-mediated hyperpolarization of [1-^{13}C, 2,3-d_2]-diethylsuccinate (32). The PHIP study of DES did, however, consistently detect a minor signal at 175.2 ppm, which is not observed in our experiments and was indicated to be fumarate. The previous work assigned the three major signals at 182.5, 177.6, and 172.7 ppm to succinate, malate and aspartate, respectively. Despite the overall similarity of the spectra, we found several inconsistencies with the previous report's assignments: (1) the chemical shifts found in the metabolite reference data did not agree with the assigned spectra (32) and (2) a single resonance was attributed to asymmetric compounds (i.e. malate and aspartate) that should display two resolvable signals due to scrambling of the ^{13}C label between the C1 and C4 positions (4027). Given these issues, we sought to reexamine the fate of [^{13}C]-DES *in vivo* and conduct a thorough study to determine the metabolite distribution.

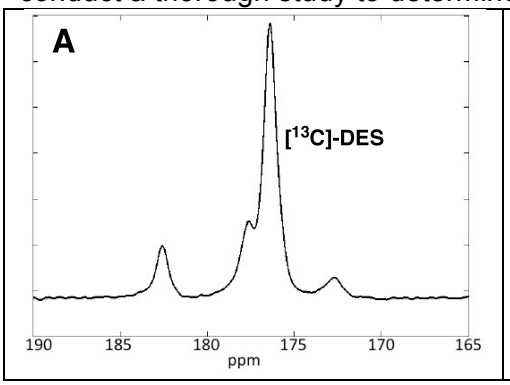

Figure 3. (A) Representative time-averaged spectra from 6 - 45 s obtained from heart beginning at the administration of 80 mM [^{13}C]-DES. (B) Representative stackplot of spectra obtained from heart at 3 s intervals beginning at the administration of 80 mM [^{13}C]-DES.

In order to evaluate whether the metabolites observed *in vivo* correspond to products of esterase cleavage (i.e.[^{13}C]-MES and/or [1,4-^{13}C]-succinate), a reference standard was prepared with a mixture of these products. A sample containing a 2:3:6 ratio of succinate:DES:MES was prepared through treating [1,4-^{13}C]-succinate with 1.0 equivalent of trimethylsilyl chloride in ethanol at room temperature (Figure 4). The ratio of metabolites was determined through analysis of the ^{1}H-NMR of the sample. This standard was then used to reference the MES and succinate carbonyl shifts via ^{13}C-NMR on an 11.7 T NMR instrument. Both [1,4-^{13}C]-succinate (183.7 ppm) and [^{13}C]-DES (176.4 ppm) yield a single resonance as they are symmetric molecules. It was discovered that peaks 182.5 and 177.6 ppm correspond to [^{13}C]-MES and do not originate from metabolism via the TCA cycle (Figure 3B). Based upon the difference in chemical shifts, [1,4-^{13}C]-succinate should be resolvable *in vivo* from the signal corresponding to [4-^{13}C]-MES, so we conclude that [1,4-^{13}C]-succinate is not forming in detectable quantities during the time frame of the *in vivo* experiment.

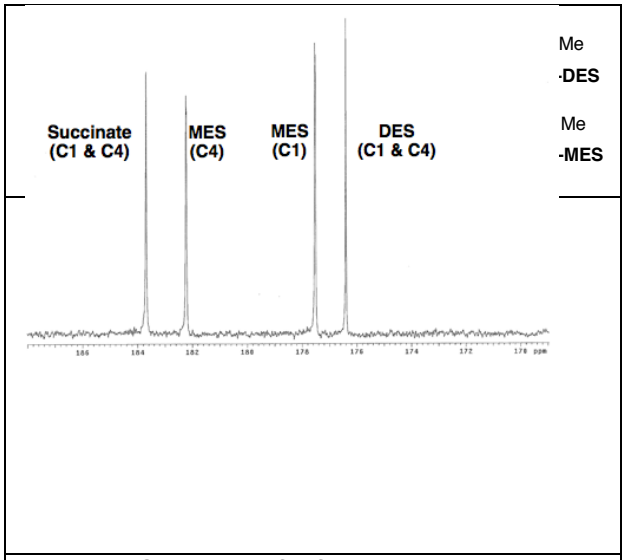

Figure 4. Synthesis of reference sample containing succinate, DES and MES. ^{13}C-NMR spectrum displays the relative chemical shift of these compounds.

DES was developed as agent for hyperpolarized ^{13}C metabolic imaging because it was hypothesized to cross biological membranes more readily than the parent compound. However, given that esterases are known to be present in the blood (4128), we sought to examine whether cleavage of [^{13}C]-DES to [^{13}C]-MES could occur extracellularly prior to entry into the cytosol or mitochondria. In order to initially confirm that [^{13}C]-DES was a substrate for esterases, the substrate was incubated with pig liver esterase. As anticipated, [^{13}C]-MES was cleanly formed and two signals (182.5 and 177.6 ppm) were observed. Next, [^{13}C]-DES was added to a freshly drawn rat blood sample, and [^{13}C]-MES was again rapidly formed in the first 5 min (Figure 5). No signal corresponding to the unknown compound (172.7 ppm) was detected under these conditions.

In order to determine the identity of this unknown metabolite, we sought to generate, isolate and characterize the species via *in vitro* methods. [^{13}C]-DES was incubated with homogenates of rat heart tissue. In all trials, conversion to [^{13}C]-MES was observed. However, only trace levels of the unknown metabolite at 172.7 ppm were detected, and unfortunately, the product could not be successfully characterized via this process. Furthermore, prostate cancer cells (PC-3) were dosed with [^{13}C]-DES (10 mM), but no metabolic product corresponding to the signal at 172.7 ppm was observed (see supporting information).

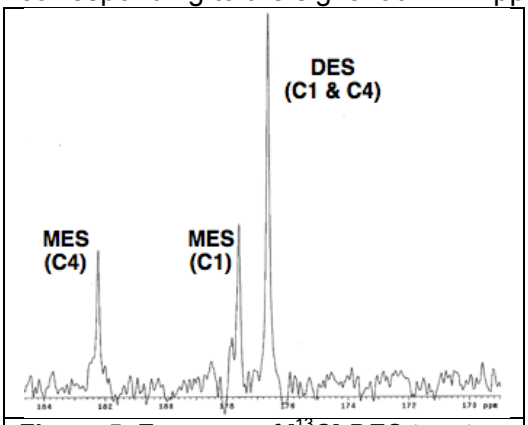

Figure 5. Exposure of [^{13}C]-DES to rat blood. Representative spectrum (20 min) shown to display the conversion to [^{13}C]-MES via endogenous esterases.

In order to assign the unknown signal, a series of succinate-derived compounds were referenced and compared with previously published TCA cycle metabolites (Table 1). As described above, the signal at 172.7 ppm did not coincide with any intermediate of the TCA cycle. The chemical shifts of aspartate and glutamate, which are products typically formed from TCA cycle intermediates, were also not consistent with the unknown metabolite. However, based upon this analysis, the unknown species in the *in vivo* spectra was assigned to [1,4-^{13}C]-succinic anhydride. This assignment was also in agreement with the fact that only a single resonance is observed, which would be expected from a symmetrical molecule like [1,4-^{13}C]-succinic anhydride. In addition, [1,4-^{13}C]-succinic anhydride maintains the carbon skeleton of [^{13}C]-DES without performing any C-C bond cleavage steps, which in the TCA cycle would be associated with the loss and subsequent observation of [^{13}C]-CO_2 at 125 ppm, which is in fast exchange with [^{13}C]-bicarbonate at 161 ppm. Neither resonance was observed in the *in vivo* experiment.

Succinate would be expected to have a relatively slow rate of dehydration under normal physiological conditions (4229-4330); therefore, it is unlikely that [1,4-^{13}C]-succinate converts to [1,4-^{13}C]-succinic anhydride. However, monoesters of succinate have been shown to be unstable due to the close proximity of the neighboring carboxyl group (44). Although the precise mechanism of the formation of [1,4-^{13}C]-succinic anhydride remains unclear, this process could potentially be enzyme- or esterase-mediated from [^{13}C]-MES. Upon formation, [1,4-^{13}C]-succinic anhydride should slowly hydrolyze to furnish [1,4-^{13}C]-succinate, which may then be metabolized by the TCA cycle but is not observed at detectable levels in our experiments.

In conclusion, although the diester analog, [^{13}C]-DES, of [^{13}C]-succinate is more adept at crossing cellular membranes, the substrate is not successfully metabolized by the TCA cycle. [^{13}C]-DES is initially metabolized to [^{13}C]-MES via endogenous esterases, which may occur in the blood rather than the intracellular environment. Further metabolism of the substrate leads to formation of [1,4-^{13}C]-succinic anhydride. Contrary to previous reports of PHIP hyperpolarized [^{13}C]-labeled DES, TCA cycle-derived metabolites (succinate, malate and aspartate) were not observed. Ongoing research efforts are directed towards the development of novel agents that have the ability to monitor *in vivo* TCA cycle metabolism and, in turn, address the current limitations in this field.

Key Research Accomplishments

1. Branched-chain amino acid metabolism is altered in human prostate cancer relative to healthy tissue.
2. Only low levels of BCAT activity were found in all prostate cancer animal and cellular models examined.
3. BCAT activity can be determined with hyperpolarized ^{13}C MRS *in vitro* using [1-^{13}C]-KIC, and the ratio of metabolite product to substrate ([1-^{13}C]-Leu-to-[1-^{13}C]-KIC) could be used as metric for monitoring changes in metabolic state. These spectroscopic results were further correlated with traditional *in vitro* assays.
4. Despite the fact that BCAT activity is altered in prostate cancer relative to healthy tissue, insufficient enzymatic levels significantly limits the use of this biomarker for hyperpolarized ^{13}C MR spectroscopic imaging of prostate cancer *in vivo*.
5. Although the diester analog, [^{13}C]-DES, of [^{13}C]-succinate is more adept at crossing cellular membranes, the substrate is not successfully metabolized by the TCA cycle. [^{13}C]-DES is initially metabolized to [^{13}C]-MES via endogenous esterases, which may occur in the blood rather than the intracellular environment. Further metabolism of the substrate leads to formation of [1,4-^{13}C]-succinic anhydride.
6. Contrary to previous reports of PHIP hyperpolarized [^{13}C]-labeled DES, TCA cycle-derived metabolites (succinate, malate and aspartate) are not observed following the bolus injection of hyperpolarized [1,4-^{13}C]-diethylsuccinate.

Reportable Outcomes

1. Billingsley K, Park JM, Josan S, Hurd RE, Mayer D, Nishimura D, Brooks J, and Spielman D, "Probing Branched-Chain Amino Acid Metabolism in Prostate Cancer with Hyperpolarized [1-^{13}C]-Ketoisocaproate", under review, *International Journal of Cancer*.
2. Billingsley K, Josan S, Park JM, Tee SS, Hurd RE, Mayer D, and Spielman D, "Hyperpolarized [1,4-13C]-Diethylsuccinate: A Potential DNP Substrate for In Vivo Metabolic Imaging", under review, *Journal of the American Chemical Society.*
3. Billingsley K, Josan S, Park JM, Yen YF, Hurd RE, Mayer D, Nishimura DG, Brooks J, **Spielman D**, Branched-Chain Amino Acid Metabolism in Prostate Cancer: Hyperpolarized [1-13C]-Ketoisocaproate as a Novel Molecular Probe, Program Number: 3933, 21st ISMRM Annual Scientific Meeting, Salt Lake City, UT, 2013.
4. Billingsley K, Josan, S, Park JM, Tee SS, Yen YF, Hurd R, Mayer D, **Spielman D**, Hyperpolarized [1,4-13C]-Diethylsuccinate: A Potential DNP Substrate for in vivo Metabolic Imaging, Program Number: 3935, 21st ISMRM Annual Scientific Meeting, Salt Lake City, UT, 2013.

Conclusion

Our most significant findings to date are that hyperpolarized ^{13}C-labeled substrates targeting BCAT metabolism are unlikely to be successful for in vivo imaging of prostate cancer, and that, while hyperpolarized 1,4-^{13}C]DES had be proposed by others as a substrate for measuring TCA cycle metabolism, in vivo downstream NMR peaks produced follow the bolus injection of ^{13}C-DES do not in fact correspond to any TCA intermediates. The next phases in our research plan are to evaluate the potential for aiding prostate cancer diagnosis of hyperpolarized ^{13}C-glycerate (glucose metabolism marker) and hyperpolarized ^{13}C-cysteine (maker for oxidative stress).

References

1. Ferlay J, Shin HR, Bray F, Forman D, Mathers C, Parkin DM. GLOBOCAN 2008 v1.2, Cancer Incidence and Mortality Worldwide: IARC CancerBase No. 10 [Internet] Lyon, France: International Agency for Research on Cancer, 2010.
2. Singh H, et al. Predictors of prostate cancer after initial negative systematic 12 core biopsy. *J Urol* 2004; **171**: 1850-4.
3. Jemal A, et al. Cancer statistics. *CA Cancer J Clin* 2008; **58**: 71-96.
4. Makarov DV. Biomarkers for Prostate Cancer. *Ann Rev Med* 2009; **60**: 139-151.
5. Pound CR, et al. Natural history of progression after PSA elevation following radical prostatectomy. *JAMA* 1999; **281**: 1591-7.
6. Kirkham AP, Emberton M, Allen C. How good is MRI at detecting and characterising cancer within the prostate? *Eur Urol* 2006; **50**: 1163-74.
7. Kurhanewicz J, Vigneron DB. Advances in MR spectroscopy of the prostate. *Magn Reson Imaging Clin N Am* 2008; **16**: 697-710.
8. Jiang Z, Woda BA. Diagnostic utility of alpha-methylacyl CoA racemase (P504S) on prostate needle biopsy. *Adv Anat Pathol* 2004; **11**: 316-21.
9. Jadvar, H. Molecular imaging of prostate cancer: PET radiotracers. *AJR Am J Roentgenol* 2012; **199**: 278-291.
10. Ardenkjaer-Larsen JH, et al. Increase in signal-to-noise ratio of > 10,000 times in liquid-state NMR. *Proc Natl Acad Sci U S A* 2003; **100**: 10158-63.
11. Day SE, et al. Detecting tumor response to treatment using hyperpolarized 13C magnetic resonance imaging and spectroscopy. *Nat Med* 2007; **13**: 1382-1387.
12. Kurhanewicz J, et al. Current and potential applications of clinical 13C MR spectroscopy. *J Nucl Med* 2008; **49**: 341-4.
13. Nelson, S. Implementation and Applications of Hyperpolarized C-13 MRI in Medicine. in 16th Scientific Meeting of the International Society of Magnetic Resonance in Medicine. 2008. Toronto, Ontario, Canada.
14. Karlsson M, et al. Imaging of branched chain amino acid metabolism in tumors with hyperpolarized (13)C ketoisocaproate. *Int J Cancer* 2010; **127**: 729-736.
15. Brosna JT, et al. Branched-chain amino acids: enzyme and substrate regulation. *J. Nutr*. 2006; **136**: 207S-211S.
16. Niwa O, et al. A cDNA clone overexpressed and amplified in a mouse teratocarcinoma line. *Nucleic Acids Res*, 1990; **18**: 6709.
17. Ben-Yosef T, et al. Involvement of Myc targets in c-myc and N-myc induced human tumors. *Oncogene* 1998; **17**: 165-71.
18. Wang Q, et al. Androgen receptor and nutrient signaling pathways coordinate the demand for increased amino acid transport during prostate cancer progression. *Cancer Research* 2011; **71**: 7525-7536.
19. Baracos VE, et al. Investigations of branched-chain amino acids and their metabolites in animal models of cancer. *J Nutr* 2006; **136**: 237S-242S.
20. Blomstrand, E. Branched-chain amino acids: metabolism, physiological, function, and application. *J Nutr* 2006; **136**: 269S-273S.
21. Schuster DM, et al. Initial experience with the radiotracer anti-1-amino-3-18F-fluorocyclobutane-1-carboxylic acid with PET/CT in prostate carcinoma. *J Nucl Med* 2007; **48**: 56-63.
22. Schadewaldt P, et al. Coupled enzymatic assay for estimation of branched-chain L-amino acid aminotransferase activity with 2-oxo acid substrates. *Anal Biochem* 1996; **238**: 65–71.
23. Sobel RE, et al. Cell lines used in prostate cancer research: a compendium of old and new lines. *J Urol* 2005; **173**: 342-59.
24. Dakubo GD, et al. Altered metabolism and mitochondrial genome in prostate cancer. *J Clin Pathol* 2006; **59**: 10-16.
25. Zacharias NM, Chan HR, Sallasuta N, Ross BD, Bhattacharya P. Real-time molecular imaging of tricarboxylic acid cycle metabolism in vivo by hyperpolarized 1-13C diethyl succinate. *J. Am. Chem. Soc.* 2012; **134**: 934-943.

26. Yen Y-F, Nagasawa K.; Nakada T. Promising application of dynamic nuclear polarization for in vivo 13C MR imaging. *Mag. Reson. Med. Sci.* 2011; **10**: 211-217.
27. Ager DJ, Prakash I. Pig liver esterase catalyzed hydrolyses of diesters. A new route to the syntheses of achiral half-esters. *Synth. Commun.* 1995; **25**: 739-742.
28. Merritt ME, Harrison C, Sherry AD, Malloy CR, Burgess SC. Flux through hepatic pyruvate carboxylase and phosphoenolpyruvate carboxykinase detected by hyperpolarized 13C magnetic resonance. *Proc. Natl. Acad. Sci. U.S.A.* 2011; **108**: 19084-19089.
29. Rudakova EV, Boltneva NP, Makhaeva GF. Comparative analysis of esterase activities of human, mouse, and rat blood. *Bull. Exp. Biol. Med.* 2011; **152**: 73-75.
30. Higuchi T, Miki T. Reversible formation of amides from free carboxylic acid and amine in aqueous solution. A case of neighboring group facilitation. *J. Am. Chem. Soc.* 1961; **83**: 3899-3901.
31. Chen H-T, Chang J-G, Musaev DG, Lin MC. Computational study on kinetics and mechanisms of unimolecular decomposition of succinic acid and its anhydride. *J. Phys. Chem. A* 2008; **112**: 6621-6629.
32. Dörwald FZ. *Side Reactions in Organic Synthesis*, Wiley-VCH: Weinheim, 2005 and reference therein.

Appendix

Statement of Work – Revised 4/4/2013

Previous Task 1: Optimization of MRS data acquisition and processing for the quantitative in vivo measurement of hyperpolarized ^{13}C-KIC to ^{13}C-Leu conversion (months 1-12):

1a. Development of quantitative multislice pulse sequence and initial testing (months 1-3).
1b. In vivo validation of multislice pulse sequence, 6 TRAMP mice (months 4-5).
1c. Dose escalation study to determine minimum KIC dose that achieve saturated enzyme kinetics, 6 TRAMP mice (months 7-12).

Status: completed. We successfully developed and tested a quantitative multislice pulse sequence for measuring hyperpolarized 13C-KIC and its down stream product 13C-Leu. The formulation and sequence was tested using the TRAMP mouse model, however, no in vivo KIC-Leu conversion was observed in the tumors (independent of KIC dose).

Previous Task 2: Determine the correlation of ^{13}C-MRS detected KIC-to-leucine production rate with tumor grade (months 13-24):

2a. MRI/MRS scanning of 12 TRAMP mice (6 w/ high grade tumors, 6 w/ low grade tumors) and 6 normal control mice (months 13-20).
2b. Histological sample preparation and analysis (months 14-20).
2c. Quantitative real-time PCR for determination of enzyme expression levels (months 14-20).
2d. Data analysis and hypothesis testing (months 21-22).
2e. Manuscript preparation (months 23-24).

Status: partially completed. In vivo metabolic images and tissue assays demonstrated that the TRAMP model exhibited low BCAT activity, making this model a poor choice for these studies. Subsequent studies of several prostate cancer cell lines, identified PC-3 as having the highest BCAT activity, but still too low for adequate in vivo imaging. Subsequent assay results from human prostate cancer showed only minimal elevation of BCAT activity in the cancers as compared to normal human prostate.

Previous Task 3: Evaluate ^{13}C-MRS detected ^{13}C-KIC-to-^{13}C-Leu production rate as a biomarker for therapy monitoring using a castration model (months 25-36):

3a. MRI/MRS scanning of 12 TRAMP mice (6 castrated animals w/ high grade tumors, 6 w/ high grade tumors) and 6 normal control mice (months 25-32).
3b. Histological sample preparation and analysis (months 26-32).
3c. Quantitative real-time PCR for determination of enzyme expression levels (months 26-32).
3d. Data analysis and hypothesis testing (months 33-34).
3e. Manuscript preparation (months 35-36).

Status: abandoned

<u>New Task</u>

Task 4: Evaluate three new hyperpolarizable substrates for the assessment of prostate cancer metabolism. Specifically,

4a. [1,4-^{13}C]diethylsuccinate for the assessment of TCA cycle activity.
4b. [1-^{13}C]glycerate for the assessment of glycolysis and PKM2 activity.
4c. [1-^{13}C]cysteine as a marker for tissue redox state and oxidative stress.

Optimum formulations and doses will be determined for each of these agents, evaluated on PC-3, DU-145, LNCaP and LAPC-4 prostate cancer cell lines and xenographs, and then tested in vivo in the TRAMP mouse model.